



OPEN Naringin attenuates angiotensin II induced cardiac hypertrophy by inhibiting carbonic anhydrase II

Mahendra Mahadevaswamy¹, G. P. Suchitha², S. R. Pavan³, H. K. Vivek⁴, S. D. Nithya¹, S. Chandan⁵, Shashanka K. Prasad⁵, T. S. Keshava Prasad², Sheikh F. Ahmad¹, Sabry M. Attia⁶, Shobha Dagamajalu²✉ & Jalahalli M. Siddesha¹✉

Nutraceuticals exert a series of health benefits, including protection against cardiovascular diseases. In this study, naringin, naringenin, and quercetin were tested for their safety and efficacy in ameliorating angiotensin (Ang) II-induced cardiac hypertrophy through carbonic anhydrase II (CA-II) inhibition. *In silico* molecular docking and MD simulations exhibited that naringin strongly binds CA-II with a docking score of -9.55 kcal/mol and hydrogen bonding energy of -6.07 kcal/mol. Naringin formed stable hydrogen bond interactions with Asn62, Trp5, and N-acetyl His4 via catalytic water molecule, and a continuous interaction via major water bridge with N-acetyl His4, His4, and Trp5. Moreover, naringin effectively inhibited CA-II activity with an IC_{50} value of 82.99 ± 4.92 nM, followed by naringenin and quercetin. Of note, all the tested nutraceuticals were found to be safe as evident from the cell viability assays. Further, naringin effectively attenuated cardiac hypertrophy, as indicated by the reductions in the Ang II-induced increases in cell surface area of H9c2 cardio myoblasts ($165.6 \pm 1.26\%$ Ang II vs. $109.8 \pm 1.88\%$ Ang II + naringin), followed by naringenin and quercetin. Furthermore, naringin significantly inhibited CA-II activity ($191.77 \pm 7.69\%$ Ang II vs. $120.16 \pm 5.52\%$ Ang II + naringin) and suppressed Ang II-induced CA-II and Na^+/H^+ exchanger 1 (NHE1) protein expression. Besides, naringin suppressed Ang II-induced CA-II, NHE1, Na^+/Ca^{2+} exchanger 1 (NCX1), and angiotensin-converting enzyme (ACE1) mRNA expression. Collectively, naringin when compared to naringenin and quercetin effectively attenuated Ang II-induced cardio myoblast hypertrophy, CA-II activity, CA-II, and NHE1 expression. The naringin-mediated attenuation of cardiac hypertrophy might be through the inhibition of CA-II enzyme activity, and the suppression of NHE1, and NCX1.

Keywords Cardiac hypertrophy, NCX1, NHE1, CA-II, Nutraceuticals, Naringin

Cardiovascular diseases account for the increased morbidity and mortality in India and worldwide. Globally, the three biggest causes of increased mortality are myocardial infarction, stroke, and heart failure¹. Hypertension-induced cardiac hypertrophy is one of the main risk factors for heart failure. Hypertension is caused by many factors, including increases in angiotensin (Ang) II levels, acid-base imbalance, sodium and calcium levels, and hyperactivity of membrane transporters, including NHE1, NCX1, and Sodium/Bicarbonate co-transporter (NBC). CA-II plays a significant role in cardiopulmonary diseases by regulating NHE1. CA-II influences NHE1 transport efficiency, with direct interaction at the C-terminal region, and regulates the NHE1 activity via phosphorylation². It has been shown that the induced expression of NHE1 augments cardiac hypertrophy and myocardial pathology³. Notably, CA-II provides substrates for the membrane transporters such as NHE1, NBC, and Anion Exchanger-3 (AE3)⁴. NHE1, involved in the uptake of intracellular Na^+ , causes an overload of Ca^{2+} ions and involved in the uptake of intracellular Na^+ , causes an overload of Ca^{2+} ions and, thus, myocardial injury. Together, the elevated cardiac NHE1 and increased CA-II activity result in heart failure^{2–5}. However, NHE1 inhibition is also a sensible strategy to attenuate cardiac remodelling. However, a clinical trial reported a higher

¹Division of Biochemistry, School of Life Sciences, JSS Academy of Higher Education & Research, SS Nagar, Mysuru 570015, India. ²Center for Systems Biology and Molecular Medicine, Yenepoya Research Centre, Yenepoya (Deemed to be University), Mangalore 575018, India. ³Yenepoya Research Centre, Yenepoya (Deemed to be University), Mangalore 575018, India. ⁴Department of Biotechnology, Adichunchanagiri School of Natural Sciences, ACU-CRI, Adichunchanagiri University, B. G. Nagara, Karnataka 571448, India. ⁵Department of Biotechnology & Bioinformatics, JSS Academy of Higher Education & Research, SS Nagar, Mysuru 570015, India. ⁶Department of Pharmacology and Toxicology, College of Pharmacy, King Saud University, Riyadh 11451, Saudi Arabia. ✉email: shobha_d@yenepoya.edu.in; siddeshajm@jssuni.edu.in

incidence of mortality and cerebrovascular side effects with direct NHE1 inhibition⁶. Moreover, CA-II is a key enzyme that regulates NHE1 activity and provides the substrate for a transporter. Of note is that the inhibition of CA-II activity might indirectly suppress NHE1 activity and contribute to the reduced risk of heart diseases. The CA-II inhibition decreases inflammation and cardiac hypertrophy⁴. However, considering the adverse effects of the existing CA-II inhibitory drugs^{7,8}. It is imperative to develop effective and safer nutraceutical-based treatment strategies for cardiovascular diseases. Multiple studies have shown that nutraceuticals, including quercetin, naringenin, and its glycoside component naringin, offer substantial protective effects against various cardiovascular diseases, including myocardial ischemia and cardiac hypertrophy^{9,10}. Martinez et al. reported that nutraceuticals such as quercetin, naringenin and genistein showed direct cardiovascular actions. Testai et al. (2013) demonstrated that naringenin provides direct cardioprotective effects against damage caused by severe ischemia/reperfusion in Langendorff-perfused rat hearts¹¹. Hence, in this study, we aim to test the nutraceuticals naringin, naringenin, and quercetin for their safety and efficacy as CA-II inhibitors, followed by evaluating their efficiency in attenuating angiotensin II-induced cardio myoblast hypertrophy using H9c2 cells.

Results
Molecular Docking

Naringin, naringenin, and quercetin exhibited similar interactions with CA-II compared to acetazolamide, a standard CA-II inhibitor. Among the docked nutraceuticals, naringin exhibited the highest docking score of -9.55 kcal/mol with a greater hydrogen bonding energy of -6.07 kcal/mol (Table 1). Besides, naringin binds well with NHE1, while naringenin and quercetin bind loosely to CA-II. These data suggest that naringin strongly interacts with the CA-II and NHE1 compared to naringenin and quercetin. However, in case of NHE1, naringin binds comparatively more efficiently with a docking score of -7.93 kcal/mol (Table 1). Of note, naringin exhibited a similar extent of binding as compared to acetazolamide (Table 1). Further, MM/GBSA was performed for all the docked complexes to validate the molecular docking findings.

MM/GBSA

The MMGBSA data of $\Delta G_{(binding\ energy)}$, $\Delta G_{(Coulomb)}$, $\Delta G_{(Covalent\ energy)}$, $\Delta G_{(H-bond)}$, $\Delta G_{(Lipo)}$, and $\Delta G_{(vdW)}$ are given in Table 1. Naringin showed an acceptable G_{total} and hydrogen bond score. However, the total $\Delta G_{(total\ binding\ energy)}$ was found to be superior (-29.83 kcal/mol) against CA-II among the tested nutraceuticals (Table 1). Naringenin and quercetin showed the least binding with CA-II. It is worth noting that similar observations were reflected in the case of NHE1 with less efficiency, as represented in Table 1. The more coulombic forces and Van der Waals forces are observed to be governed by naringin during interaction with CA-II. However, in case of NHE1, Van der Waals forces contributed more to binding with naringin. Hence, CA-II complexed with naringin, naringenin, quercetin, and acetazolamide were analysed to understand the naringin-CA-II complex stability and interaction strength by molecular dynamics.

*Standard CA-II inhibitor drug.

Molecular dynamics simulations

RMSD is one of the fundamental factors which is used to estimate protein stability compared to the initial structure. RMSF analysis was performed to evaluate the average fluctuations of residues during the simulation. In this study, naringin formed stable interactions with CA-II throughout 200 ns, and protein RMSD and ligand RMSD fluctuated within the limit ranging from 1-2.2Å. In the first phase of the interaction, protein RMSD was found to be stable throughout 200 ns, and ligand RMSD fluctuated from 10 ns to 130 ns (Fig. 1a). Herein, the seventh oxygen atom of naringin showed bonding with Asn62 and Asn61 of CA-II (Fig. 1b and e). Based on these observations, it is confirmed that the naringin and CA-II form stable complex throughout molecular dynamic simulations. The two-dimensional pictorial representation exhibits hydrogen bonds between naringin and amino acid residues Asn62, Trp5, and N-acetyl His4 (ACE3) of CA-II *via* a catalytic water molecule (Fig. 1b and d). The L-RMSF plot of naringin with CA-II shows that oxygen atoms 7, 9, and 14 form active interactions with strengths of 32%, 59%, and 30%, respectively (Fig. 1b and c) and with Glu69 with bond strength of 31%. Naringin forms a major water bridge with His4, Trp5, and Asn62, which is a continuous interaction (Fig. 1e),

Protein	Ligands	Molecular docking (kcal/mol)		MMGBSA $\Delta G_{(Bind)}$ (kcal/mol)					
		Docking Score	XP H _{Bond}	Total	Coulomb	H _{Bond}	Lipo	Packing	vdW
Carbonic anhydrase II (PDB: 1A42)	Naringin	-9.55	-6.07	-29.83	-40.98	-4.25	-8.31	-0.51	-25.61
	Naringenin	-6.08	-1.81	9.29	-29.11	-1.52	-4.57	-3.17	-30.21
	Quercetin	-5.98	-1.73	11.68	-8.66	-1.36	-10.09	-2.52	-31.20
	*Acetazolamide	-2.18	-0.54	-11.65	-18.71	-1.53	-4.23	-1.35	-26.68
NHE1 (PDB:7DSX)	Naringin	-7.93	-2.75	-25.89	-16.52	-2.76	-16.49	-2.43	-40.95
	Quercetin	-6.77	-1.79	-25.39	-9.99	-2.19	-12.43	-3.17	-26.12
	Naringenin	-6.07	-1.00	-28.11	-15.06	-1.68	-12.16	-2.71	-19.67
	*Acetazolamide	-2.20	-1.00	-15.83	-17.47	-2.24	-3.08	-1.98	-26.07

Table 1. Molecular Docking and molecular mechanics data of Naringin, naringenin, Quercetin and Acetazolamide.

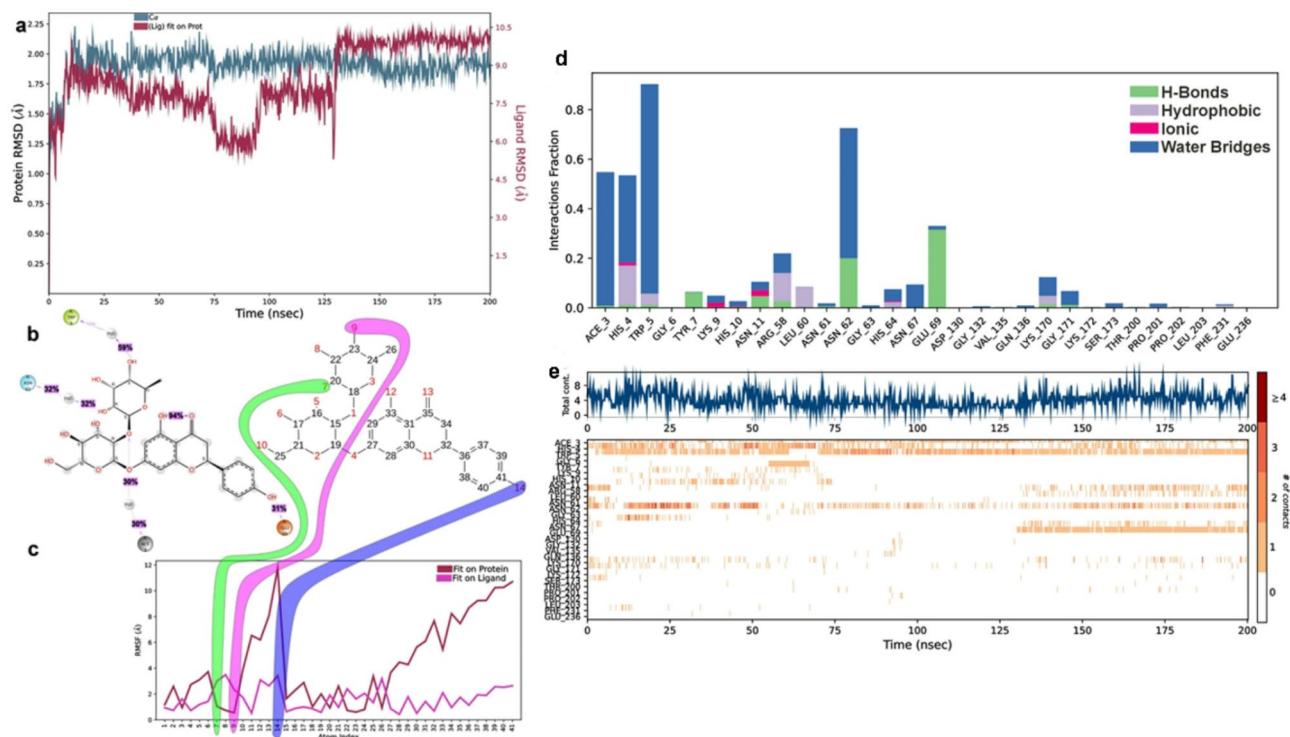


Fig. 1. Molecular dynamics simulations of naringin with CA-II. **(a)** RMSD of naringin and CA-II complex, giving insight into its structural conformation throughout the simulation, showing fluctuation within the acceptable limit. **(b)** 2D geometrical interactive plot showing interactions of amino acids with naringin. **(c)** L-RMSF depicting the interaction of naringin atoms (given in percentage) with CA-II throughout the MDSs. **(d)** Summary of the interactions of CA-II-naringin complex in a normalized stacked bar chart. **(e)** The contact strengths between the putative binding site amino acids of CA-II with naringin throughout the MDS's up to 200ns.

and the number of contact points is represented in color-coded form (Fig. 1e). Naringin forms hydrogen bonds with Asn67 and Glu69. Hence, the catalytic water molecules play a vital role in holding naringin in the putative binding site of CA-II.

Naringenin also formed stable interactions and hydrogen bonds with Asn62, Trp5, and ACE3 of CA-II via a catalytic water molecule (Figure S1a and S1b). The L-RMSF plot of naringenin with CA-II showed that the oxygen atoms 1, 2, 3, and 5 form active interactions with strengths of 42%, 33%, 32%, and 42%, respectively (Figure S1c). Of note, naringenin formed a major hydrophobic interaction with Tyr7 and Ala65 and hydrogen bonding with Asn62, His64, and Glu92, which is a continuous interaction (Figure S1d), and the contact points are represented in color-coded form (Figure S1e). The RMSD of quercetin and CA-II exhibited a stable complex (Figure S2a), having hydrogen bonds with ACE3 and Gln36 (Figure S2b). The L-RMSF plot of quercetin with CA-II showed that oxygen atoms 4 and 6 form active interactions with strengths of 33% and 36%, respectively (Figure S2c). Quercetin formed hydrophobic interactions with Tyr7 and Ala65, hydrogen bond, and water bridge with ACE3 and Gln92, which is a continuous interaction (Figure S2d), and the contact points are represented in color-coded form (Figure S2e).

Notably, RMSD of acetazolamide and CA-II remained stable with a strong interaction between the nitrogen of acetazolamide and zinc atom of CA-II active site and hydrogen bonding with Asn62, Tyr7, and Thr200 via catalytic water (Figure S3a and S3b). L-RMSF plot of acetazolamide with CA-II showed that oxygen atoms 3, 4, and 6 form active interactions with strengths of 83%, 94%, and 63%, respectively (Figure S3c). Acetazolamide formed hydrophobic interactions with Tyr7, His94, Val143, and Trp209, hydrogen bond and water bridge with Thr199 and Thr200, which is a continuous interaction (Figure S3d), and the contact points are represented in color-coded form (Figure S3e).

Collectively, *in silico* data demonstrated a strong binding affinity between naringin and CA-II with multiple interactions, including hydrogen bonding, ionic bonding, hydrophobic interactions, and water bridges. Moreover, the binding orientation of naringin was similar to that of acetazolamide, suggesting the potential of naringin as an effective CA-II inhibitor.

Carbonic anhydrase-II inhibitory activity

A series of concentration-dependent inhibition assays were performed to determine the effective enzyme inhibitory concentrations of individual molecules. Of the tested molecules, naringin and acetazolamide significantly inhibited CA-II enzyme activity at nanomolar concentrations while naringenin and quercetin

exhibited enzyme inhibitory activity at micromolar concentrations (Figure S4). Importantly, the concentrations of the tested molecules ranged from 1 nM to 1 mM, and henceforth, to ensure precise and accurate inhibitions, the varied concentrations of individual were considered. Among the tested nutraceuticals, naringin efficiently inhibited CA-II activity with an IC_{50} value of 82.99 ± 4.92 nM (Fig. 2a). The inhibitory efficiency of naringin is comparable, yet higher than acetazolamide, a standard CA-II inhibitor (IC_{50} value 26.23 ± 0.376 nM; Fig. 2b), followed by naringenin and quercetin (IC_{50} values of 68.95 ± 0.56 μ M and 70.44 ± 2.50 μ M respectively) (Fig. 2c and d). Further, these nutraceuticals were tested for their toxicity and effects on Ang II-induced cell hypertrophy.

Cell viability

Cell viability analysis of naringin, naringenin, and quercetin did not show cytotoxicity in H9c2 cells (Fig. 3a–c), which is similar to that of acetazolamide and losartan (Figure S5a–b). The cells treated with angiotensin II alone (Figure S5c) showed 87% viability at its concentration of 200nM. Of note, naringin, naringenin, quercetin (80 μ M), acetazolamide, and losartan (60 μ M) were found to be protective, and thus, these doses were considered for the evaluation; thus, these doses were considered to evaluate hypertrophy parameters.

Cardio myoblast hypertrophy

Naringin, naringenin, quercetin, and standard drugs were tested for their efficacy in attenuating Ang II-induced cardio myoblast hypertrophy. Of note, Ang II-induced cell hypertrophy, as indicated by the increased cell surface area ($165.6 \pm 1.26\%$ vs. 100% control). Besides, naringin effectively attenuated Ang II-induced hypertrophy ($109.8 \pm 1.88\%$ vs. $165.6 \pm 1.26\%$), followed by naringenin ($115.15 \pm 1.46\%$), which is similar to that of losartan ($106.87 \pm 1.69\%$). However, acetazolamide and quercetin exhibited moderate effects on Ang II-induced cell hypertrophy ($126.36 \pm 1.8\%$ and $132.37 \pm 2.53\%$ respectively) when compared to naringin and naringenin (Fig. 4).

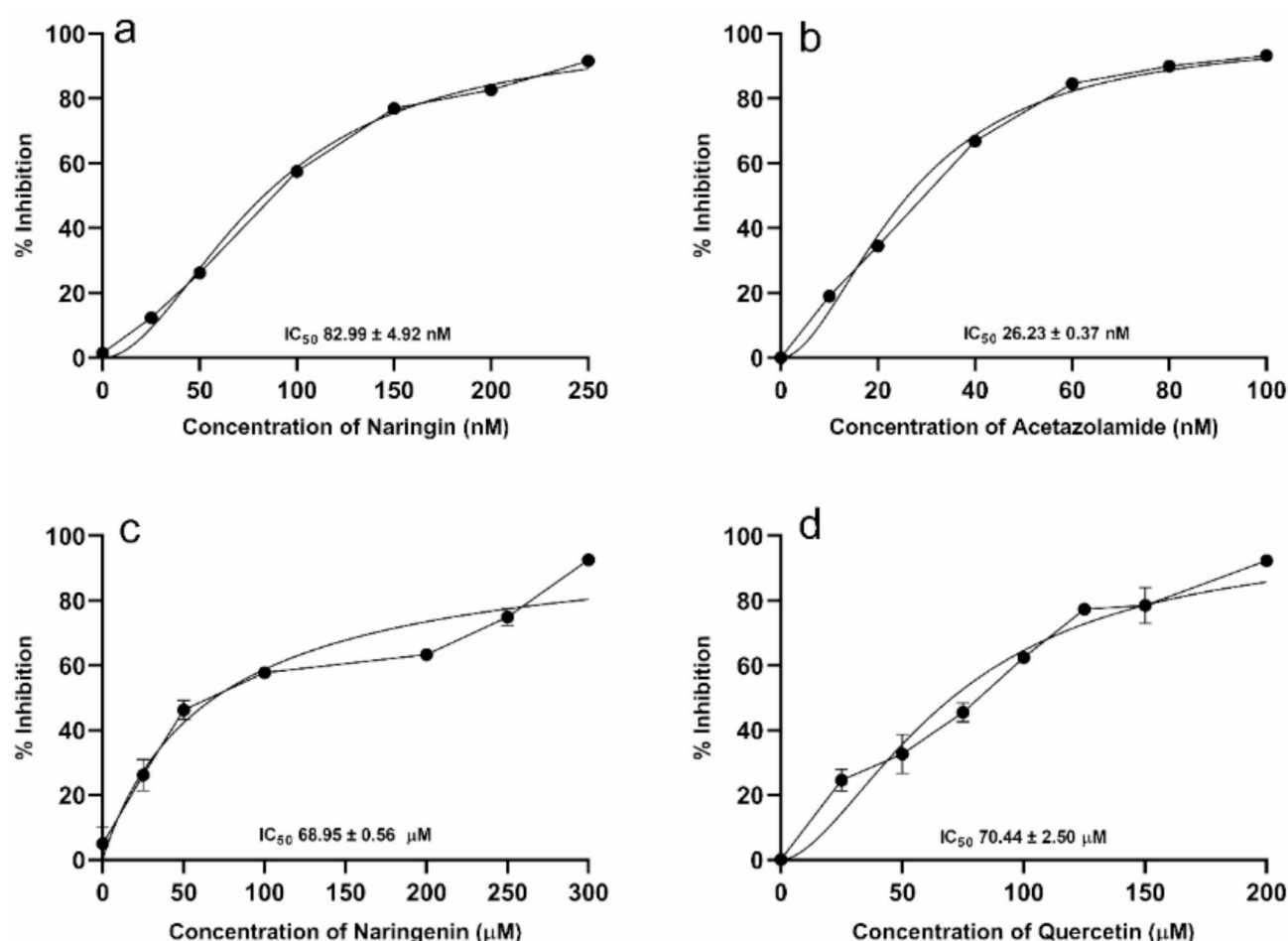


Fig. 2. Concentration-dependent inhibition of CA-II by nutraceuticals (a) naringin, (b) acetazolamide, (c) naringenin and (d) quercetin. The decreased concentration of P-nitrophenol in the test reaction compared to control and enzyme activity reaction was expressed as percentage of CA-II inhibition. Data represents mean \pm SEM ($n=3$).

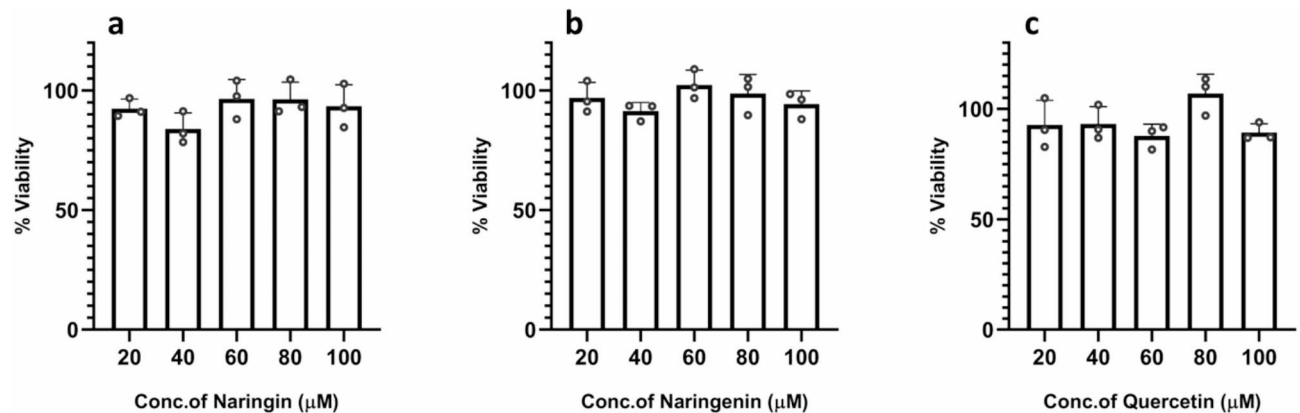


Fig. 3. Dose-dependent cytotoxicity of nutraceuticals (a) naringin, (b) naringenin, and (c) quercetin on H9c2 cells, as determined by MTT assay. Data represents mean \pm SEM ($n=3$) (* $p < 0.05$, ** $p < 0.01$, *** $p < 0.001$).

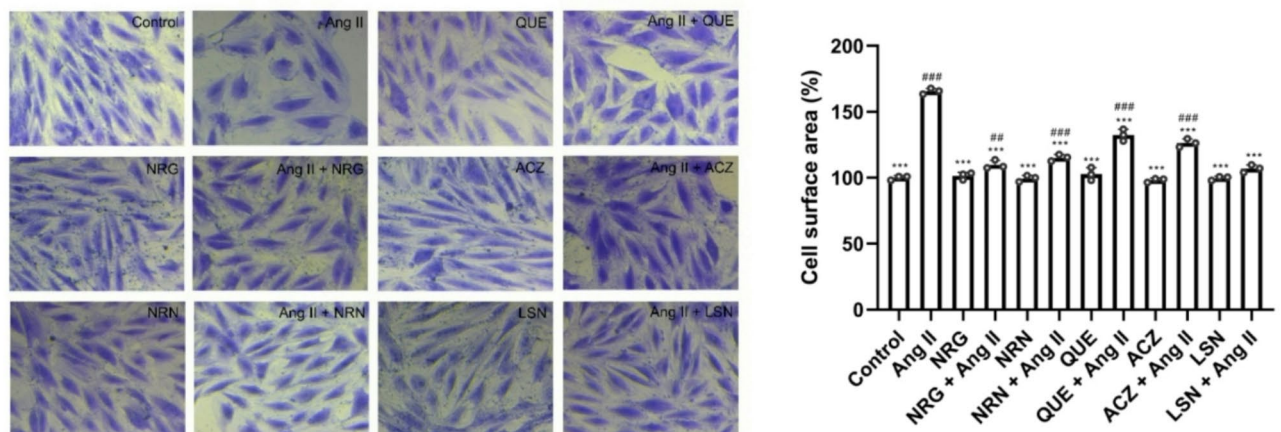


Fig. 4. Attenuation of Ang II-induced cell hypertrophy by nutraceuticals, as measured by the surface area of H9c2 cells. Cell surface area represented as mean value \pm SEM ($n=3$) (# vs. control group; * vs. Ang II group; * $P, 0.05$, ** $P, 0.01$, *** $P, 0.001$).

Carbonic anhydrase-II activity

The effect of nutraceuticals on CA-II activity in Ang II-induced cardiac hypertrophy were analysed. Ang II-induced cell hypertrophy, as indicated by the increased CA-II activity ($191.77 \pm 7.69\%$ vs. 100% control). Besides, naringin effectively attenuated Ang II-induced hypertrophy ($120.16 \pm 5.52\%$ vs. $191.77 \pm 7.69\%$), followed by naringenin ($115.15 \pm 1.46\%$), which is similar to that of losartan ($106.87 \pm 1.69\%$), which is almost similar to that of standard CA-II inhibitor acetazolamide ($114.79 \pm 2.51\%$) and antihypertensive drug losartan ($111.23 \pm 4.18\%$) followed by naringenin and quercetin exhibited moderate inhibitory activity of CA-II ($133.63 \pm 11.8\%$ and $133.64 \pm 8.03\%$ respectively) when compared to controls. Naringin, acetazolamide and losartan significantly reduced Ang II-induced CA-II activity compared to other tested molecules (Fig. 5).

Immunoblotting

The expression levels of CA-II and NHE1 and the effect of nutraceuticals on CA-II and NHE1 levels were analysed using immunoblot technique. Ang II-induced group showed the increased expression levels of CA-II and NHE1 proteins when compared to control. Of note, naringin, naringenin and losartan significantly suppressed Ang II-induced CA-II expression compared to acetazolamide and quercetin (Fig. 6). Besides all the tested compounds profoundly suppressed Ang II-induced NHE1 protein expression (Fig. 6). However, naringin and naringenin significantly suppressed CA-II and NHE1 expression, similar to that of antihypertensive drug losartan, followed by acetazolamide and quercetin.

Gene expression

Ang II significantly enhanced the mRNA levels of CA-II, NHE1, NCX1, and ACE1 in H9c2 cells compared to controls. Of note, all the tested nutraceuticals significantly attenuated Ang II-induced mRNA levels. However, naringin seems more effective in suppressing Ang II-induced gene expression than naringenin and quercetin.

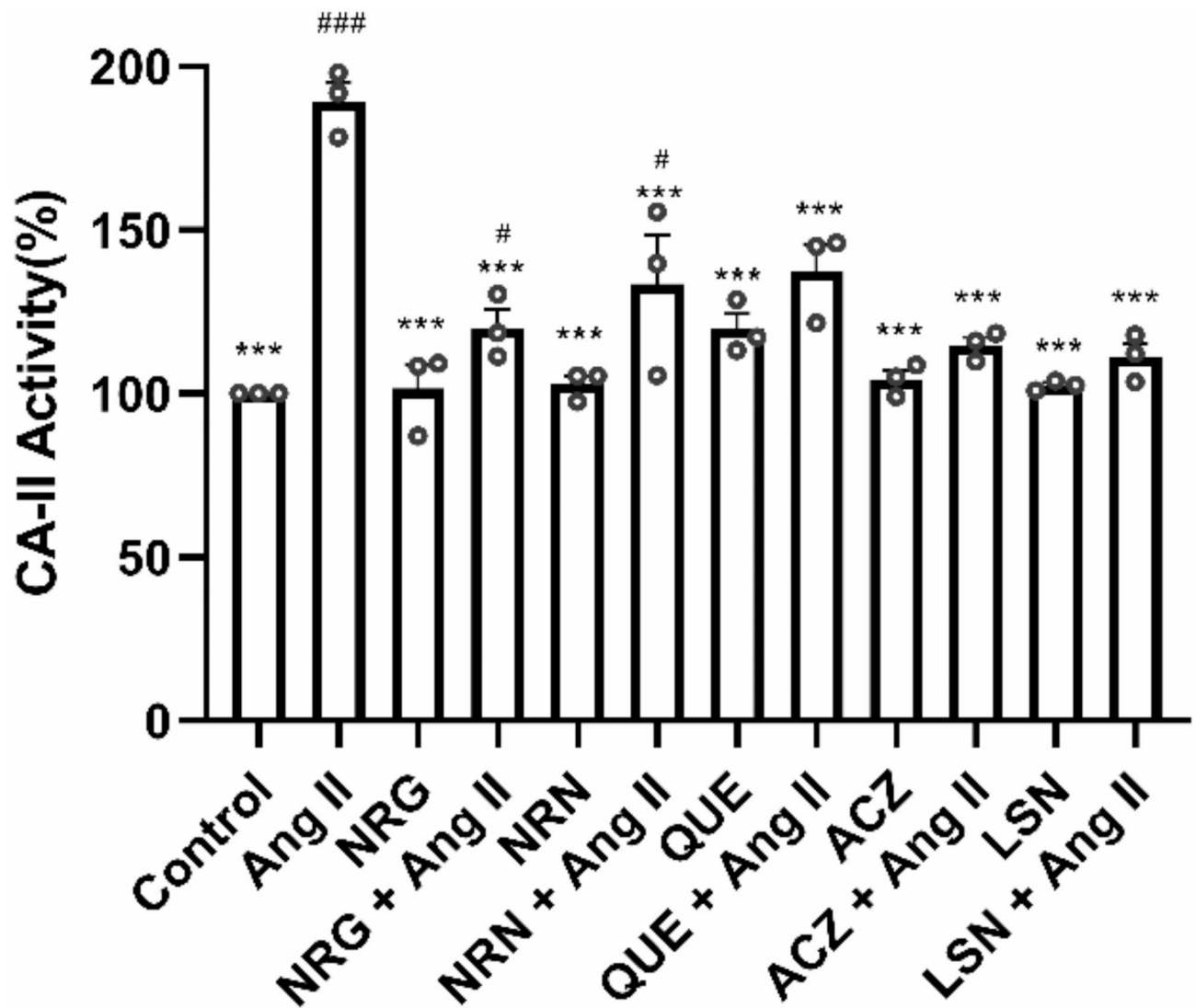


Fig. 5. Inhibition of Ang II-induced CA-II activity by nutraceuticals in H9c2 cells (# vs. control group; * vs. Ang II group; *P, 0.05, **P, 0.01, ***P, 0.001). Data represents mean \pm SEM ($n = 3$).

Besides, the effect of naringin on Ang II-induced gene expression was similar to that of losartan and acetazolamide (Fig. 7). comparison attenuated Ang II-induced cardio myoblast hypertrophy, CA-II activity mRNA, and protein expression levels of CA-II and NHE1 compared with naringenin and quercetin.

Discussion

Despite available treatment for cardiac hypertrophy and heart failure, many patients still experience disease progression, highlighting the need for additional measures¹². Importantly, nutraceuticals and dietary as well as lifestyle measures are advised due to their safety, affordability, and potential as preventive medicine¹³. So far, various nutraceuticals have been reported to alleviate oxidative and endoplasmic reticulum stress, support nitric oxide and hydrogen sulphide bioactivity, prevent cardiomyocyte pH reduction, and positively regulate cardioprotective hormones¹⁴. Moreover, nutraceuticals offer a promising approach into managing cardiac hypertrophy by targeting various pathways involved in inflammation, oxidative stress, and metabolic regulation¹³.

Of note, the flavonoids have shown potential in attenuating cardiac hypertrophy and are known for anti-inflammatory and antioxidant activities¹⁵. Importantly, the flavonoids could protect endothelial function, which is vital for maintaining cardiovascular health¹⁶. They prevent the oxidation of low-density lipoprotein and offer vasodilatory effects, helping to reduce the workload on the heart¹⁷. Quercetin has been shown to possess cardioprotective effects, including ACE inhibition, antioxidant, and anti-inflammatory properties¹⁸. Quercitrin could reduce the creation of ROS and promote the regeneration of endogenous antioxidant defences, which have been linked to the suppression of oxidative stress¹⁹. The ability of quercetin to inhibit the renin-angiotensin system (RAS) is crucial in the regulation of blood pressure and fluid balance since the overactivation of RAS leads to cardiac hypertrophy¹⁸.

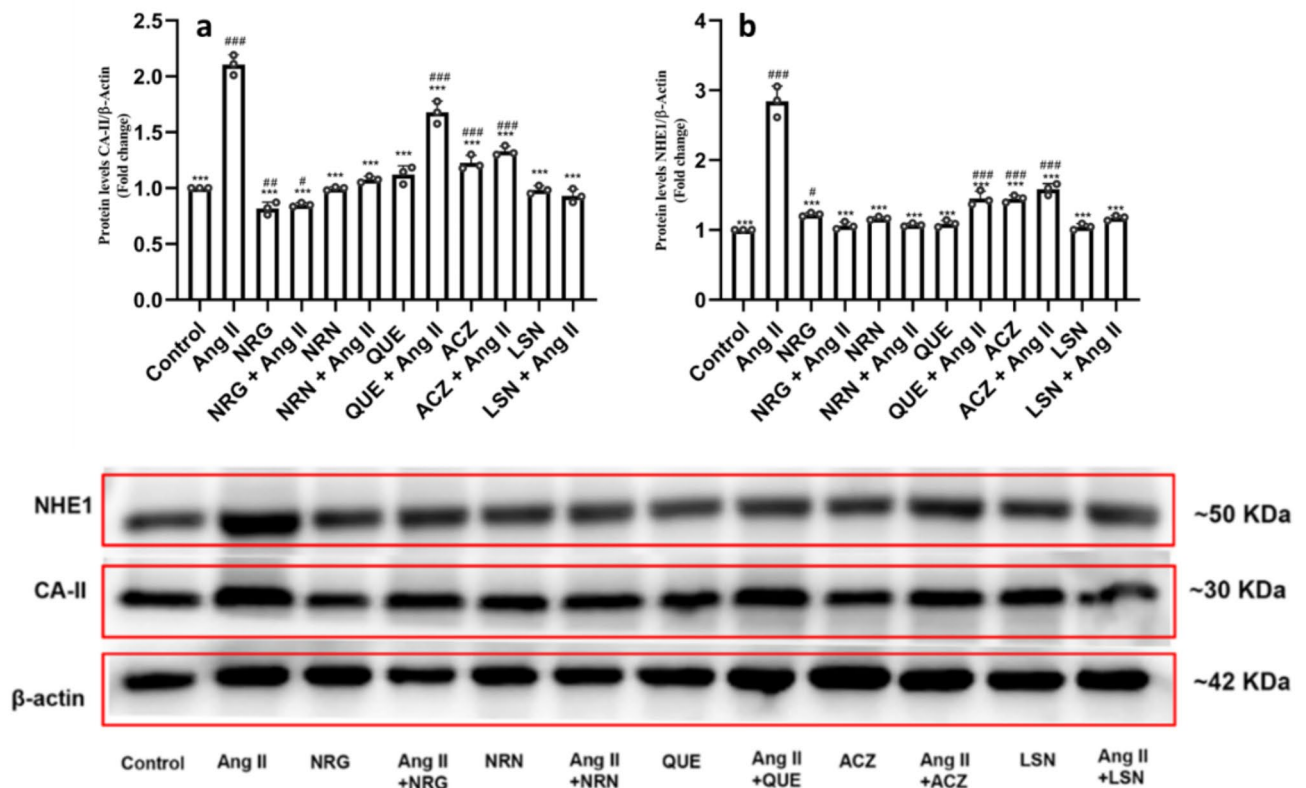


Fig. 6. Effect of nutraceuticals on CA-II and NHE1 protein expression in H9c2 cells. The β -actin served as internal control. Data represents mean \pm SEM ($n = 3$) (* vs. control group; * vs. Ang II group; * P, 0.05, ** and **P, 0.01, *** and ***P, 0.001). (Original blots/gels are presented in Supplementary Figure S6–S8)

Naringin and naringenin are also flavonoids with proven efficiency in cardioprotection. Notably, naringenin attenuates cardiac hypertrophy induced by various factors^{20,21}. For instance, naringenin can reduce oxidative stress and inhibit the AMPK/NOX2/MAPK signalling pathway, which is involved in developing cardiac hypertrophy²⁰. Additionally, naringenin has been shown to inhibit the PI3K/Akt, ERK, and JNK signalling pathways, further contributing to its cardioprotective effects²⁰. Similarly, naringin exhibits cardioprotective properties and has been shown to control the serum levels of creatinine, blood urea nitrogen, and other markers of cardiac health. Also, naringin can ameliorate cardiac toxicity and hypertrophy, displaying its importance as a preventive medicine for cardiovascular diseases²².

The literature reveals that the NHE1, NCX1, and CA-II play interconnected roles in maintaining cardiac function, and their dysregulation might contribute to an imbalance in cardiac function, including hypertrophy^{23–25}. CA-II activates the NHE1 efflux through the interaction with the C-terminal of NHE1 and donates H^+ ion as a substrate for NHE1^{26,27}. NHE1 activity affects intracellular pH, which in turn influences NCX1 function²³. The changes in intracellular pH can modulate NCX1 activity, affecting Ca^{2+} homeostasis^{28,29}. Thus, the intricate relationship between NHE1, NCX1, and CA-II might impact cardiac contractility, arrhythmogenesis, and overall cellular homeostasis.

In this study, quercetin, naringenin, and naringin showed a higher affinity towards CA-II. MD simulation results suggested the similarity between naringin and acetazolamide in their binding pattern, binding regions, and bonding interactions. The MM/GBSA score is important in validating in silico molecular docking data, and the bioactivity data set is typically linked with MM/GBSA scores¹³. Of note, G_{score} was calculated to validate molecular docking results and predict the protein-ligand complex's behavior. Naringin showed a sufficient G_{score} and hydrogen bond score and higher binding energy than other compounds. Naringenin and quercetin showed the least binding with CA-II. It is worth noting that similar observations were reflected in the case of NHE1 with less efficiency, as represented.

MDSs were employed to study the molecular dynamics of a docked complex of ligands against the targeted macromolecule. The molecular docking analyses revealed that the naringin formed stable interactions with CA-II via four ionic bonds, nine hydrogen bonds, and six hydrophobic interactions. In contrast, acetazolamide formed four ionic bonds, four hydrogen bonds, and four hydrophobic interactions. Moreover, the binding mode of naringin was similar to that of acetazolamide. On the other hand, naringenin and quercetin formed four and seven hydrogen bonds respectively, with CA-II, and did not form ionic bonds. However, naringenin and quercetin had three and two hydrophobic interactions with CA-II, respectively. Importantly, naringin and acetazolamide were similar in making ionic and hydrogen bonding and showed similar binding modes.

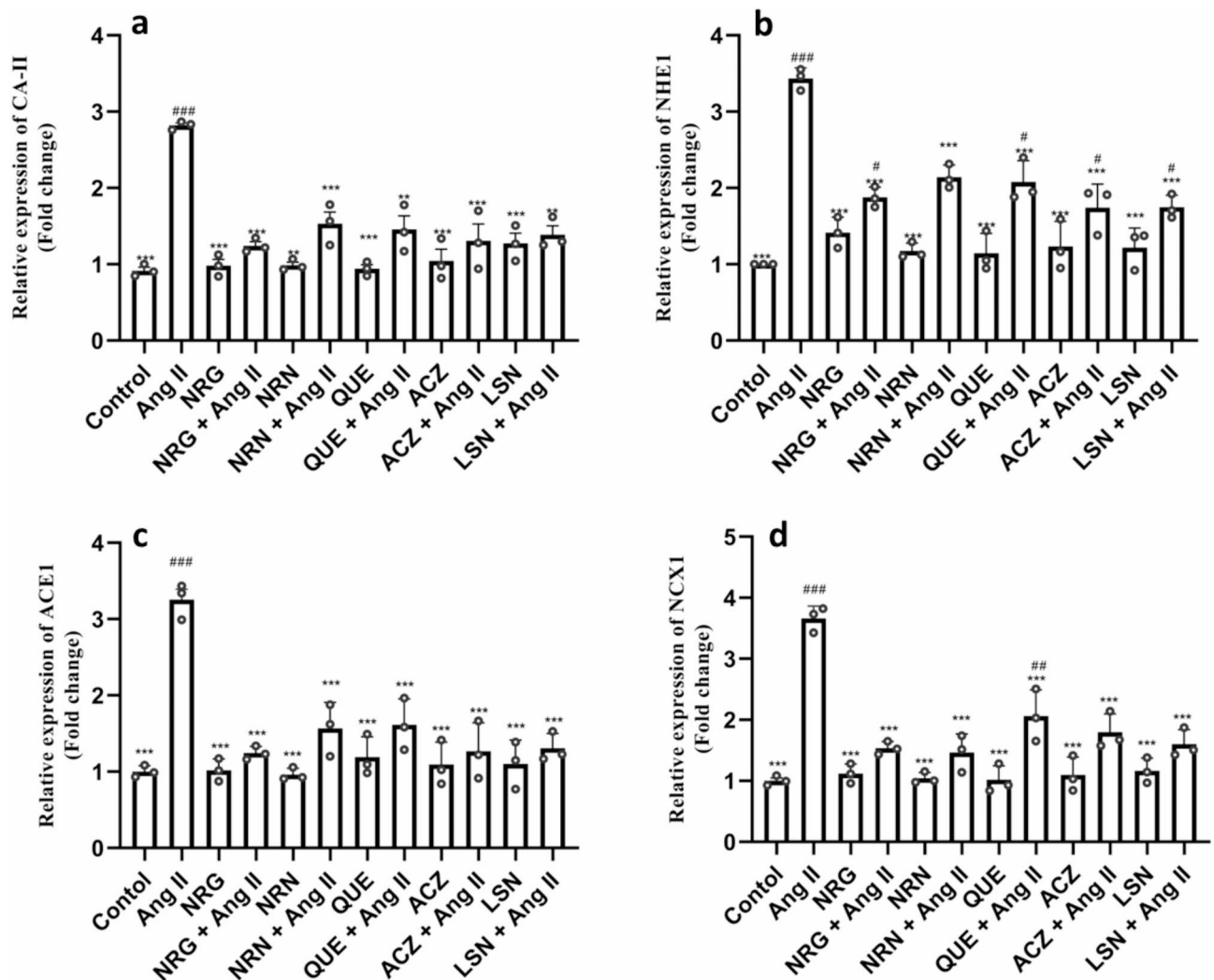


Fig. 7. Effect of nutraceuticals on (a) CA-II, (b) NHE1, (c) NCX1, and (d) ACE1 gene expression in H9c2 cells. The β -actin served as internal control. Data represents mean \pm SEM ($n = 3$). Data represents mean \pm SEM ($n = 3$) (# vs. control group; * vs. Ang II group; * $P, 0.05$, # and ** $P, 0.01$, *** and *** $P, 0.001$).

Overall, the in-silico data confirmed a strong binding affinity of naringin for CA-II and the similarity in binding orientations of naringin and acetazolamide with CA-II.

In this study, we tested naringin, naringenin, quercetin along with acetazolamide for their CA-II inhibitory efficacy in vitro and demonstrated their efficacy in attenuating cardiac hypertrophy in comparison with losartan in H9c2 cells. Acetazolamide, a standard CA-II inhibitor is widely used as diuretic drug in humans^{30,31} and losartan, an angiotensin II receptor blocker exert antihypertensive effects through distinct mechanisms³². The antihypertensive mechanism of acetazolamide involves the reduction of sodium bicarbonate reabsorption in the kidney³³. This leads to loss of bicarbonate in the urine, pulling water along with it, reducing plasma volume and extracellular fluid volume, thus lowering blood pressure^{33,34}. On the other hand, losartan exerts antihypertensive effect by blocking angiotensin II binding to the AT1 receptor, thus suppressing angiotensin II-mediated effects including vasoconstriction, systemic vascular resistance and aldosterone secretion. Together, losartan reduces hypertension by decreasing sodium and water retention, blood volume and preload³². Remarkably, naringin exhibited higher inhibitory potential with an IC_{50} value at a nanomolar concentration, comparable with the standard CA-II inhibitor acetazolamide. In contrast, quercetin and naringenin were effective at micromolar concentrations. Of note, previously, the studies have also reported similar CA-II inhibitory effects of naringin and quercetin^{35,36}.

Previously, naringin exhibited the cardioprotective effects against anoxia/reoxygenation injury at a concentration of 40 $\mu\text{g/mL}$ (equivalent to 68.90 μM) in H9c2 cells³⁷, while 80 μM of naringenin protected against hypoxia/reoxygenation injury in cardiomyocytes³⁸. In another study, 30 μM and 100 μM quercetin demonstrated cardioprotection against oxidative stress-induced cell death, with no cardiotoxic effects observed even at higher concentrations³⁹. Considering the safety, efficacy, and preliminary standardization, the nutraceutical concentrations of 80 μM were tested in H9c2 cells. Importantly, 80 μM naringin, naringenin, and quercetin did not display toxicity against H9c2 cells, which is also evident from other studies^{37,38,40}. Further, Ang II-induced

hypertrophy model using H9c2 cardio myoblasts⁴¹ was considered for testing the effects of these nutraceuticals and standard drugs. Notably, naringin attenuated Ang II-induced cell hypertrophy, and the effect was similar to that of losartan, while superior to acetazolamide, naringenin, and quercetin. Moreover, the drug treatment alone did not show increases in cell hypertrophy or cell death, suggesting the safety and efficacy of naringin in the attenuation of cardiac hypertrophy.

It has been shown that the pro-hypertrophic agonist Ang II acts on G-protein-coupled receptors⁴², which in turn activates protein kinase C and indirectly stimulates NHE1 via mitogen-activated protein kinase⁴³. Besides, the catalytic activity of CA-II generates and provides H^+ ions to NHE1, thus stimulating the efflux action of NHE1. Of note, NHE1 activation eventually led to the rise in cytosolic Na^+ ions⁴⁴, which compromises or reverses the ability of Na^+ / Ca^{2+} exchanger1 (NCX1). Physiologically, NCX1 is involved in the efflux of Ca^{2+} ions, driven by the transmembrane Na^+ ion gradient. However, the dysregulated NCX1 increases intracellular Ca^{2+} levels and activates calcineurin, eventually contributing to the development of cardiac hypertrophy and heart failure (Fig. 8)^{45–47}.

To decipher the mode of action of nutraceuticals, the cell lysates were evaluated for both the protein and mRNA expression levels of CA-II and their counterparts. Importantly, the cell lysates of Ang II-induced hypertrophic cells exhibited significant increases in CA-II enzyme activity. However, Ang II-induced increases in CA-II enzyme activity were effectively inhibited by naringin. Likewise, naringenin and quercetin moderately inhibited CA-II enzyme activity. Of note, the observed enzyme inhibitory efficiency of naringin was similar to acetazolamide and losartan. It is critical to understand that the CA-II regulates NHE1 and NCX1, thus contributing to cardiac hypertrophy². Hence, the Ang II-induced expression levels of CA-II and NHE1 proteins and the effect of nutraceuticals on Ang II-induced CA-II and NHE1 protein levels were analysed. Importantly, Ang II increased CA-II and NHE1 protein levels, while naringin and losartan significantly suppressed Ang II-induced CA-II protein expression. On the other hand, naringenin efficiently suppressed Ang II-induced NHE1 protein expression, followed by naringin, losartan, quercetin, and acetazolamide.

Lastly, the mRNA expression analyses were undertaken to comprehend the nutraceutical-mediated molecular mechanisms. It is known that CA-II, NHE1, and NCX1 interplay, as well as ACE1 expression, play a key role in

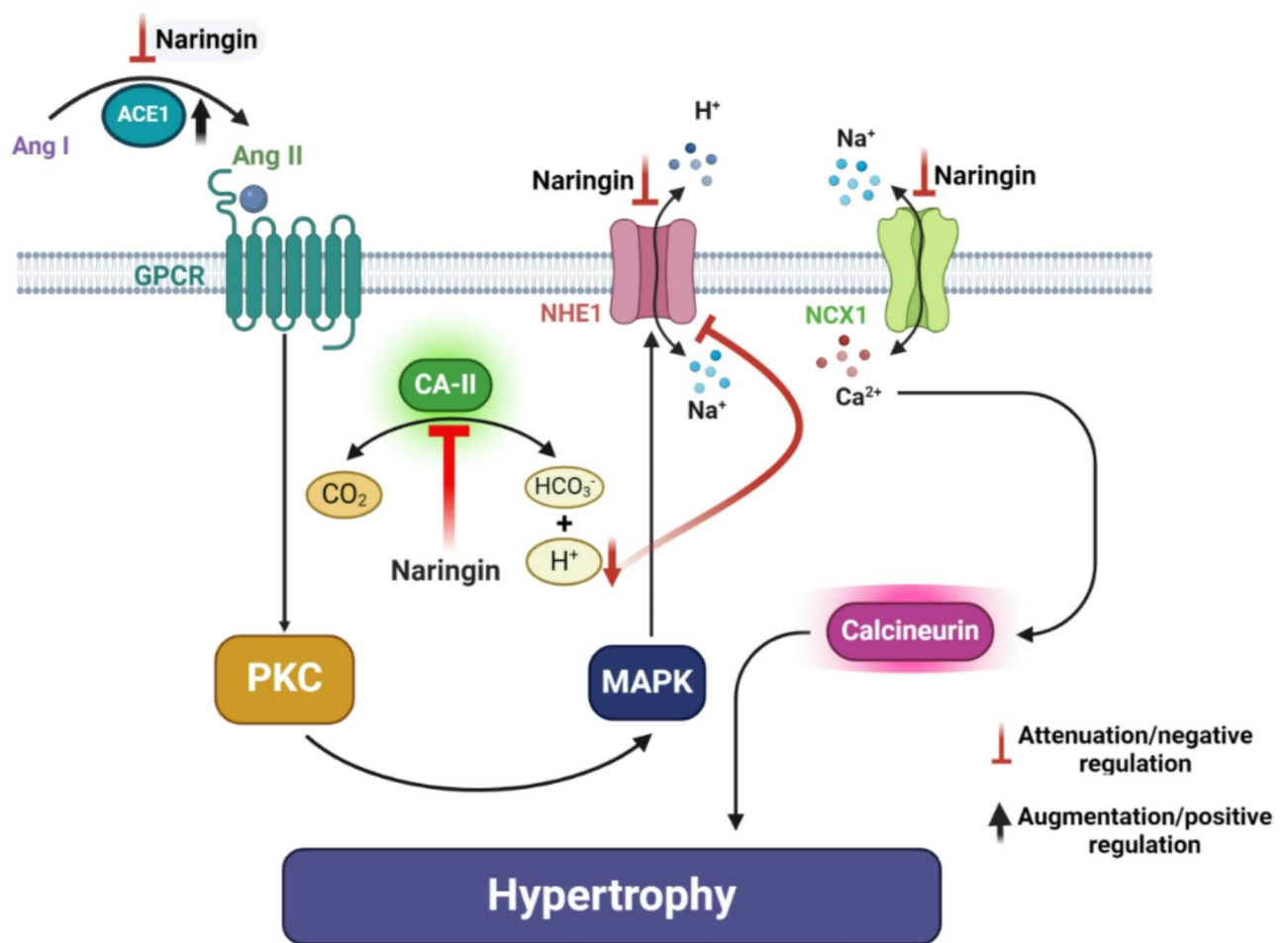


Fig. 8. Schema showing possible mechanisms of actions of naringin on CA-II-mediated signal transduction pathways involved in the development of Ang II-induced cardiac hypertrophy, via negative regulation of CA-II, NHE1, NCX1 and ACE1.

cardiac hypertrophy⁴⁸. Principally, CA-II, NHE1, NCX1, and ACE1 mRNA levels were significantly amplified in Ang II-infused hypertrophic cells. Though, all the tested nutraceuticals attenuated Ang II-induced mRNA levels, naringin alone was found to be effective and similar to that of losartan and acetazolamide. Collectively, naringin might have inhibited CA-II enzyme activity either through direct interaction with CA-II protein or regulation of mRNA and protein expression levels of CA-II. Furthermore, naringin-mediated regulation of CA-II expression and enzyme activity along with the suppression of NHE1, NCX1, and ACE1 might have collectively contributed to the attenuation of Ang II-induced cardiac hypertrophy (Fig. 8).

Conclusions

Naringin, naringenin, and quercetin were found to be safe and effective at 80 μ M concentrations in ameliorating Ang II-induced cardio myoblast hypertrophy. Of note, nutraceutical-mediated attenuation of cardio myoblast hypertrophy corresponds to the inhibition of CA-II enzyme activity and suppression of CA-II and NHE1 expression. Perhaps, nutraceutical-mediated effects might be through the suppression of CA-II-mediated signal transduction pathways involved in the development of Ang II-induced cardiac hypertrophy, via negative regulation of CA-II, NHE1, NCX1 and ACE1.

Materials and methods

Materials

Carbonic anhydrase II (Cat# C2522-5MG), Quercetin (Cat# 1592409), naringin (Cat# N1376-25G), naringenin (Cat# N5893-5G), acetazolamide (Cat# A6011-10G), losartan (Cat# SML3269-10MG), angiotensin II (Cat# A9525), 4-nitrophenyl acetate (Cat. No: N8130-5G), and crystal violet (Cat# 61135) were obtained from Sigma (St. Louis, MO, USA). Nitrocellulose membrane (Cat# 1620115) and ECL substrate (Cat. No: 1705060) were obtained from BioRad Laboratories (USA). MTT assay kit (Cat# CCK003-1000 LOT# 0000578578) was from HiMedia Laboratories Pvt Ltd (Bengaluru, India), DMEM medium (Cat# 12100046), FBS (Cat# A3160801), penicillin, and streptomycin (Cat# 10378016) from Gibco (Grand Island, NY, USA). Internal control β -actin (Cat#4967, LOT #ZC385732), Primary antibodies for CA-II (Cat# MA5-49145 LOT#ZA4177591) and Nhe-1 (Cat# PA5-116471, LOT #ZA4173385B), secondary antibodies, goat anti-mouse IgG2b (Cat# A-21242, LOT #2465093), and goat anti-rabbit IgG (Cat# 32460 LOT #YK383320), and BCA assay kit (Cat#23235) were from Thermo Fisher Scientific (Waltham, MA, USA). Prime Script RT Reagent (Cat# RR037A LOT#AN51001N) and TB Green[®] Premix Ex Taq II (Tli RNaseHPlus) (Cat# RR820A LOT #AN41007N) obtained from TaKaRa (Shiga, Japan). All primers were from Integrated DNA Technologies (Singapore).

Molecular Docking

The in-silico docking methods were performed as described previously by Jiang et al.⁴⁹. CA-II (PDB ID: 1A42)⁵⁰ and NHE1 (PDB ID: 7DSX)⁵¹ Were retrieved from the Protein Data Bank (PDB). Each protein was constructed using automated default parameters, ensuring accurate bond configurations and charge assignments. The protein preparation involved the retention of catalytic water molecules and the application of an OPLS3 force field for the minimization⁵². A root-mean-square deviation (RMSD) of 0.30 Å was set for heavy atom convergence before docking in Maestro's Prime module, and a receptor grid of 30 Å was generated. Structures of naringin, naringenin, quercetin and acetazolamide were imported from the PubChem database. Energy minimization was performed with OPLS3 for each ligand, followed by extra-precision docking to evaluate docking scores⁵³.

MM/GBSA calculation

Molecular mechanics with generalized Born and surface area solvation (MM/GBSA) is a widely used technique to estimate the free energy associated with binding small ligands to biological macromolecules. It lies between rigorous alchemical perturbation approaches and empirical scoring functions regarding accuracy and computational complexity. MM/GBSA was employed to predict binding free energies (ΔG_{bind}) of quercetin, naringin, naringenin, and acetazolamide to CA-II and NHE1⁵⁴. The docked complex structures were visualized using the pose viewer, and the results were analyzed using the Prime MM/GBSA module in Maestro, force field OPLS3 and VSGB 2.0 solvation model was used in Maestro to predict ΔG_{bind} ⁵⁵. The binding free energy was calculated using the minimized energies of the receptor, ligand, and receptor-ligand complex, using the equation below to calculate ΔG_{bind} .

$$\Delta G(\text{bind}) = E_{\text{complex}}(\text{minimized}) - [E_{\text{ligand}}(\text{minimized}) + E_{\text{receptor}}(\text{minimized})]$$

Molecular dynamic simulations (MDSs)

The MDSs were performed on a 64-bit Ubuntu 20.04 system using the Maëstro software. The docking scores for CA-II with ligands, validated through MM/GBSA, were utilized in the MDSs. The protein-ligand complex was solubilized using the TIP3P water model by employing the system-builder option within an orthorhombic periodic boundary box. To achieve charge neutrality, Hg^{2+} ions (2.403 mM), Cl^- ions (52.875 mM), and Na^+ ions (50.472 mM) were added. The default relaxation method from the Desmond program was applied for MDSs, maintaining several atoms, pressure, and temperature under NPT ensemble conditions at 310 K and 1 atmosphere. The analysis focused on root mean square deviation (RMSD), root mean square fluctuation (RMSF), and total energy of the complexes, utilizing event analysis and simulation-interaction diagrams over a simulation period of 200 nanoseconds^{56,57}.

CA-II inhibitory assay

p-nitrophenyl acetate, a synthetic substrate, is hydrolyzed by CA-II to create p-nitrophenol, which exhibits an absorption peak at 405 nm. The generation of p-nitrophenol enables colourimetric detection of the product

and subsequent estimation of CA-II activity⁵⁷. In summary, a 96-well plate was filled with triplicate solutions of 1.26 U/180 µl of CA-II in the presence or absence of inhibitors and 3 mM of p-nitrophenol acetate. The reaction buffer contained 50 mM TrisSO₄, pH 7.6, and a final volume of 180 µl. The changes in the absorbance at 405 nm following a 30-minute incubation period at 25 °C were detected and recorded using a Multiskan™ FC Microplate photometer. The maximal activity obtained without an inhibitor was considered 100% activity and used to define the % inhibition. IC₅₀ values were computed from a graph of per cent inhibition vs. inhibitor concentration using GraphPad Prism 8.0 software.

Cell culture

H9c2 embryonic rat heart-derived cells were obtained from NCCS, Pune. The cells cultured in DMEM medium were enriched with 10% FBS, 3.7 g/L NaHCO₃, and antibiotics (streptomycin at 100 µg/ml, penicillin at 100 U/ml). Cells were maintained in a humidified incubator with an atmosphere of 95% oxygen and 5% carbon dioxide. For various assays, the cells were seeded at different densities: 0.5×10^4 cells per well in 96-well plates for cell viability tests, 3×10^4 cells in 24-well plates for crystal violet staining and surface measurement, and 1×10^6 cells in 6-well plates for extracting proteins and mRNA.

Cell viability assay

The MTT assay was performed to analyze the effects of the test compounds. For this, a density of 0.5×10^4 cells per well was seeded in 96-well plates, allowing the culture plate to get 70–85% confluence. Once cells are confluent, they were exposed to different concentrations of quercetin, naringenin, and naringin and standard CA-II inhibitor acetazolamide, antihypertensive drug losartan (20, 40, 60, 80, and 100 µM), and Ang II at (50, 100, 150, 200, and 250 nM). Acetazolamide and nutraceuticals were dissolved in a final DMSO concentration of less than 0.1% (v/v). Control cells received the same dosage of DMSO as a vehicle. The control and treated cells were incubated for 48 h. Then, MTT solution (1 mg/mL) was added to each well at a volume of 70 µL and incubated for 3 to 4 h. Afterwards, the media was discarded, and 200 µL of DMSO and ethanol (50:50) was added to each well to dissolve the formazan crystals. The plates were then gently shaken at room temperature for 5 to 10 min and the absorbance was measured at 570 nm by a multimode plate reader (Multiskan Sky, Thermo Fisher Scientific). The percentage of cell viability was calculated as the relative absorbance of the treated cells vs. untreated control cells⁵⁸.

Cell surface area measurement

Crystal violet staining of H9c2 cardio myoblasts was employed as previously reported, with slight modifications⁴¹. Briefly, treated cardiomyoblasts were rinsed 2–3 times with PBS, incubated with 3% crystal violet dissolved in methanol for 1 h at room temperature, and washed the wells with PBS until the stain was removed. Then, the cardiomyoblasts were observed under a light microscope. The cross-sectional area of at least 100 representative cells from each experimental group was quantified using microscopic images captured from randomly selected fields. The measurements were performed using ImageJ software.

Protein extraction

Cells were seeded into a 10 cm dish at a density of 2.5×10^5 . Dishes were grouped into 12 groups: control, Ang II (200 nM) alone; nutraceutical (quercetin, naringenin, and naringin; 80 µM) alone; nutraceutical with Ang II, acetazolamide (60 µM) alone, acetazolamide with Ang II, losartan (60 µM) alone, and losartan with Ang II. The cells were then harvested in cell lysis buffer [4% sodium dodecyl sulfate in 50 mM triethylammonium bicarbonate, with 1 mM sodium orthovanadate, 2.5 mM sodium pyrophosphatase, and 1 mM beta-glycerophosphate] after 48 h and cells were lysed by sonication on ice with discontinuous disruption at 30% amplification. The cells were centrifuged at 12,000 g for 30 min at 4°C, supernatants were transferred to sterile tubes and stored at -20 °C for further experiments⁵⁹.

Protein expression studies

Protein concentration was estimated using a BCA protein estimation kit. The protein (20 µg) samples were loaded onto SDS- PAGE (NHE1- 10% gel and CA II 12% gel, respectively) for the western blot analyses. The proteins were blotted using a nitrocellulose membrane and blocked with 5% BSA in 1X PBST. Next, the nitrocellulose membrane was independently incubated with primary antibodies (NHE1 and CA II – 1:500 dilutions) at 4 °C temperature overnight and then with respective HRP-conjugated secondary antibodies (1:3000 dilution) for 90 min at room temperature. The protein bands were observed using ECL substrate (Bio-Rad), and densitometry analyses were performed using ImageJ software⁵⁹. The β-actin was used as a reference control.

Gene expression studies

Cells were seeded into a 10 cm dish at a density of 2.5×10^5 . Dishes were grouped into 12 groups: control, Ang II (200 nM) alone; nutraceutical (quercetin, naringenin, and naringin; 80 µM) alone; nutraceutical with Ang II, acetazolamide (60 µM) alone, acetazolamide with Ang II, losartan (60 µM) alone, and losartan with Ang II. Total RNA was extracted from cell lysates using Tri-reagent and then reverse-transcribed into cDNA using Prime Script RT Reagent (TaKaRa) cDNA synthesis kit for CA-II, NHE1, NCX1, and ACE1 (Table 2). Reverse transcription PCR (RT-PCR) was performed using TB Green® Premix Ex Taq II (Tli RNaseHplus) SYBR Green PCR Master Mix. The β-actin serves as the reference control⁶⁰.

Statistical analysis

All data were expressed as mean ± standard error ($n=3$). Statistical analyses were conducted using GraphPad Prism 8.0 software. One-way analysis of variance (ANOVA) was used to evaluate significant difference among

Gene	Forward primer (5'-3')	Reverse primer (3'-5')
CA-II	TAAGCACCGGAAAATGGAAG	AAGCCACATACCGGCAAAC
NHE 1	CTCCAGCTCAACCCTACTGC	AGGGAGATCTCGAAGGGTGT
NCX 1	TGACCAGCAAAGAGGAGGAG	AGCTTCTCTCCCCACATTC
ACE 1	CACTGGAGCCTGATCTGACA	GGCTGCAGCTCCTGGTATAG

Table 2. List of rat primers used for RT-qPCR.

multiple groups followed by Dunnett's test^{61–63}. A value of $p < 0.05$ was considered statistically significant. * $p < 0.05$; ** $p < 0.01$; *** $p < 0.001$.

Data availability

The data could be obtained upon request to the corresponding author.

Received: 28 November 2024; Accepted: 21 March 2025

Published online: 06 April 2025

References

- Kalra, A. et al. The burgeoning cardiovascular disease epidemic in Indians – perspectives on contextual factors and potential solutions, May 01, *Elsevier Ltd.* (2023). <https://doi.org/10.1016/j.lansea.2023.100156>
- Li, X., Alvarez, B., Casey, J. R., Reithmeier, R. A. F. & Fliegel, L. Carbonic anhydrase II binds to and enhances activity of the Na⁺/H⁺ exchanger, *Journal of Biological Chemistry*, vol. 277, no. 39, pp. 36085–36091, Sep. (2002). <https://doi.org/10.1074/jbc.M111952200>
- Mraiche, F., Oka, T., Gan, X. T., Karmazyn, M. & Fliegel, L. Activated NHE1 is required to induce early cardiac hypertrophy in mice, *Basic Res Cardiol*, vol. 106, no. 4, pp. 603–616, Jul. (2011). <https://doi.org/10.1007/s00395-011-0161-4>
- Alvarez, B. V. et al. Feb., Carbonic anhydrase inhibition prevents and reverts cardiomyocyte hypertrophy, *Journal of Physiology*, vol. 579, no. 1, pp. 127–145, (2007). <https://doi.org/10.1113/jphysiol.2006.123638>
- Nakamura, T. Y., Iwata, Y., Arai, Y., Komamura, K. & Wakabayashi, S. Activation of Na⁺/H⁺ exchanger 1 is sufficient to generate Ca²⁺ signals that induce cardiac hypertrophy and heart failure, *Circ Res*, vol. 103, no. 8, pp. 891–899, Oct. (2008). <https://doi.org/10.1161/CIRCRESAHA.108.175141>
- Mentzer, R. M. et al. Apr., Sodium-Hydrogen Exchange Inhibition by Cariporide to Reduce the Risk of Ischemic Cardiac Events in Patients Undergoing Coronary Artery Bypass Grafting: Results of the EXPEDITION Study, *Annals of Thoracic Surgery*, vol. 85, no. 4, pp. 1261–1270, (2008). <https://doi.org/10.1016/j.athoracsur.2007.10.054>
- Sanah Aslam and Gupta, V. *Carbonic Anhydrase Inhibitors* (StatPearls Publishing, 2023).
- Supuran, C. T., Scozzafava, A. & Casini, A. Carbonic anhydrase inhibitors. *Mar* <https://doi.org/10.1002/med.10025> (2003).
- Yaseen, H. S. et al. Naringin: cardioprotective properties and safety profile in diabetes treatment. *Fitoterapia* **176**, 106011. <https://doi.org/10.1016/j.fitote.2024.106011> (2024).
- Galán-Martínez, L., Herrera-Estrada, I. & Fleites-Vázquez, A. Direct actions of the flavonoids naringenin, quercetin and genistein on rat cardiac and vascular muscles [Acciones directas de los flavonoides naringenina, quercetina y genisteína sobre los músculos cardíaco y vascular de rata], *J Pharm Pharmacogn Res*, vol. 6, no. 3, pp. 158–166, [Online]. (2018). Available: <http://jppres.com/jppres>
- Testai, L., Martelli, A., Cristofaro, M., Breschi, M. C. & Calderone, V. Cardioprotective effects of different flavonoids against myocardial ischaemia/reperfusion injury in Langendorff-perfused rat hearts. *J. Pharm. Pharmacol.* **65** (5), 750–756. <https://doi.org/10.1111/jphp.12032> (May 2013).
- McCarty, M. F. Nutraceutical, dietary, and lifestyle options for prevention and treatment of ventricular hypertrophy and heart failure. *Apr 01 2021 MDPI AG* <https://doi.org/10.3390/ijms22073321>
- Dama, A. et al. Targeting Metabolic Diseases: The Role of Nutraceuticals in Modulating Oxidative Stress and Inflammation, Feb. 01, *Multidisciplinary Digital Publishing Institute (MDPI)*. (2024). <https://doi.org/10.3390/nu16040507>
- Mazza, A. et al. Nutraceuticals for serum lipid and blood pressure control in hypertensive and hypercholesterolemic subjects at low cardiovascular risk. *Adv. Ther.* **32** (7), 680–690. <https://doi.org/10.1007/s12325-015-0229-x> (Jul. 2015).
- Gupta, L., Chauhan, M., Kumar, A., Chauhan, D. & Saini, P. Flavonoids and cardiovascular diseases, in *Advances in Flavonoids for Human Health and Prevention of Diseases*, Apple Academic, 73–94. doi: <https://doi.org/10.3109/13880200490893483>. (2024).
- Choy, K. W. et al. Flavonoids as natural anti-inflammatory agents targeting nuclear factor-kappa B (NFκB) signaling in cardiovascular diseases: A mini review, *Front Pharmacol*, vol. 10, no. OCT, (2019). <https://doi.org/10.3389/fphar.2019.01295>
- Kozłowska, A. & Szostak-Węgierek, D. Targeting Cardiovascular Diseases by Flavonols: An Update, Apr. 01, *MDPI*. (2022). <https://doi.org/10.3390/nu14071439>
- Dmello, J. R., Chandekar, L. P., Bavadekar, T. A., Buttar, H. S. & Kaur, G. Quercetin: A promising flavonoid for the therapy of cardiac hypertrophy and heart failure mediated by the Renin angiotensin system, in *The Renin Angiotensin System in Cardiovascular Disease*, (eds Dhalla, N. S., Bhullar, S. K. & Shah, A. K.) Cham: Springer International Publishing, 377–405. doi: https://doi.org/10.1007/978-3-031-14952-8_23. (2023).
- Charachit, N., Sukhamwang, A., Dejkiengkraikul, P. & Yodkeeree, S. Hyperoside and Quercitrin in houttuynia cordata extract attenuate UVB-Induced human keratinocyte cell damage and oxidative stress via modulation of MAPKs and Akt signaling pathway. *Antioxidants* **11** (2). <https://doi.org/10.3390/antiox11020221> (Feb. 2022).
- Li, Y. et al. Naringenin attenuates Isoprenaline-Induced cardiac hypertrophy by suppressing oxidative stress through the AMPK/NOX2/MAPK signaling pathway. *Nutrients* **15** (6). <https://doi.org/10.3390/nu15061340> (Mar. 2023).
- Zhang, N. et al. Dec., Naringenin attenuates pressure overload-induced cardiac hypertrophy, *Exp Ther Med*, vol. 10, no. 6, pp. 2206–2212, (2015). <https://doi.org/10.3892/etm.2015.2816>
- Shackebaei, D. et al. Cardioprotective effect of naringin against the ischemia/reperfusion injury of aged rats. *Naunyn Schmiedeberg Arch. Pharmacol.* **397** (2), 1209–1218. <https://doi.org/10.1007/s00210-023-02692-2> (2024).
- Tóth, A. & Varró, A. Role of NCX1 and NHE1 in ventricular arrhythmia, in *Heart Rate and Rhythm: Molecular Basis, Pharmacological Modulation and Clinical Implications*, (eds Tripathi, O. N., Quinn, T. A. & Ravens, U.) Cham: Springer International Publishing, 293–307. doi: https://doi.org/10.1007/978-3-031-33588-4_13. (2023).
- Watanabe, Y. Cardiac Na⁺/Ca²⁺ exchange stimulators among cardioprotective drugs, Nov. 01, *Springer*. (2019). <https://doi.org/10.1007/s12576-019-00721-5>

25. Herrmann, S. et al. Sep., The cardiac sodium-calcium exchanger NCX1 is a key player in the initiation and maintenance of a stable heart rhythm. *Cardiovasc Res*, vol. 99, no. 4, pp. 780–788, (2013). <https://doi.org/10.1093/cvr/cvt154>
26. Sjøgaard-Frich, L. M. et al. Mar., Dynamic Na⁺/H⁺ exchanger 1 (NHE1) - calmodulin complexes of varying stoichiometry and structure regulate Ca²⁺-dependent NHE1 activation, *Elife*, vol. 10, (2021). <https://doi.org/10.7554/eLife.60889>
27. Vallés, P. G., Bocanegra, V., Gil Lorenzo, A. & Costantino, V. V. Physiological Functions and Regulation of the Na⁺/H⁺ Exchanger [NHE1] in Renal Tubule Epithelial Cells, Aug. 22, S. Karger AG. (2015). <https://doi.org/10.1159/000368521>
28. Magi, S. et al. Intracellular calcium and ischemic damage: dual role of the Na⁺/Ca²⁺ Exchanger, in The First Outstanding 50 Years of Università Politecnica Delle Marche: Research Achievements in Life Sciences, (eds Longhi, S., Monteriù, A., Freddi, A., Aquilanti, L., Ceravolo, M. G., Carnevali, O., Giordano, M. & Moroncini, G.) Cham: Springer International Publishing, 361–372. doi: https://doi.org/10.1007/978-3-030-33832-9_24. (2020).
29. Chou, A. C., Ten Ju, Y. & Pan, C. Y. Calmodulin interacts with the sodium/calcium exchanger NCX1 to regulate activity. *PLoS One*. **10** (9). <https://doi.org/10.1371/journal.pone.0138856> (Sep. 2015).
30. Claude, A. Diuretics, in *Pharmacology in Veterinary Anesthesia and Analgesia*, pp. 315–323. (2024). <https://doi.org/10.1002/9781118975169.ch24>
31. Sabina, M., Barakat, Z., Feliciano, A., Lamb, A. & Alsamman, M. M. Unlocking the Potential of Acetazolamide: A Literature Review of an Adjunctive Approach in Heart Failure Management, Jan. 01, *Multidisciplinary Digital Publishing Institute (MDPI)*. (2024). <https://doi.org/10.3390/jcm13010288>
32. Li, D. et al. Binding of Losartan to Angiotensin AT1 Receptors Increases Dopamine D1 Receptor Activation, *Journal of the American Society of Nephrology*, vol. 23, no. 3, [Online]. (2012). Available: https://journals.lww.com/jasn/fulltext/2012/03000/binding_of_losartan_to_angiotensin_at1_receptors.11.aspx
33. Koeppen, B. M. The kidney and acid-base regulation. *Adv. Physiol. Educ.* **33**, 275–281. <https://doi.org/10.1152/advan.00054.2009> (2009).
34. Eskandari, D., Zou, D., Grote, L., Hoff, E. & Hedner, J. Acetazolamide reduces blood pressure and sleep-disordered breathing in patients with hypertension and obstructive sleep apnea: A randomized controlled trial, *Journal of Clinical Sleep Medicine*, vol. 14, no. 3, pp. 309–317, Mar. (2018). <https://doi.org/10.5664/jcsm.6968>
35. Taslimi, P., Caglayan, C. & Gulcin, I. The impact of some natural phenolic compounds on carbonic anhydrase, acetylcholinesterase, butyrylcholinesterase, and α -glycosidase enzymes: an antidiabetic, anticholinergic, and antiepileptic study. *J. Biochem. Mol. Toxicol.* **31** (12). <https://doi.org/10.1002/jbt.21995> (Dec. 2017).
36. Ekinci, D. et al. Carbonic anhydrase inhibitors: In vitro inhibition of α isoforms (hCA I, hCA IV) by flavonoids, *J Enzyme Inhib Med Chem*, vol. 28, no. 2, pp. 283–288, (2013). <https://doi.org/10.3109/14756366.2011.643303>
37. Chen, R. C., Sun, G. B., Wang, J., Zhang, H. J. & Sun, X. B. Naringin protects against anoxia/reoxygenation-induced apoptosis in H9c2 cells via the Nrf2 signaling pathway, *Food Funct*, vol. 6, no. 4, pp. 1331–1344, Apr. (2015). <https://doi.org/10.1039/c4fo01164c>
38. Tang, J. Y. et al. Naringenin ameliorates hypoxia/reoxygenation-induced Endoplasmic reticulum stress-mediated apoptosis in H9c2 myocardial cells: involvement in ATF6, IRE1 α and PERK signaling activation. *Mol. Cell. Biochem.* **424**, 1–2. <https://doi.org/10.1007/s11010-016-2848-1> (Jan. 2017).
39. Daubney, J., Bonner, P. L., Hargreaves, A. J. & Dickenson, J. M. Cardioprotective and cardiotoxic effects of quercetin and two of its in vivo metabolites on differentiated H9c2 cardiomyocytes, *Basic Clin Pharmacol Toxicol*, vol. 116, no. 2, pp. 96–109, Feb. (2015). <https://doi.org/10.1111/bcpt.12319>
40. Angeloni, C., Spencer, J. P. E., Leoncini, E., Biagi, P. L. & Hrelia, S. Role of Quercetin and its in vivo metabolites in protecting H9c2 cells against oxidative stress. *Biochimie* **89** (1), 73–82. <https://doi.org/10.1016/j.biochi.2006.09.006> (Jan. 2007).
41. Abdulrahman, N. et al. Empagliflozin inhibits angiotensin II-induced hypertrophy in H9c2 cardiomyoblasts through Inhibition of NHE1 expression. *Mol. Cell. Biochem.* **477** (6), 1865–1872. <https://doi.org/10.1007/s11010-022-04411-6> (Jun. 2022).
42. Zhang, X., Zhang, S., Wang, M., Chen, H. & Liu, H. Advances in the allosteric of angiotensin II type 1 receptor. *Dec. 01 2023 BioMed. Cent. Ltd.* <https://doi.org/10.1186/s13578-023-01063-x>
43. Verma, K., Pant, M., Paliwal, S., Dwivedi, J. & Sharma, S. An Insight on Multicentric Signaling of Angiotensin II in Cardiovascular system: A Recent Update, Aug. 20, *Frontiers Media S.A.* (2021). <https://doi.org/10.3389/fphar.2021.734917>
44. Fliegel, L. Role of Genetic Mutations of the Na⁺/H⁺ Exchanger Isoform 1, in Human Disease and Protein Targeting and Activity, Feb. 01, *Springer*. (2021). <https://doi.org/10.1007/s11010-020-03984-4>
45. Bers, D. M., Barry, W. H. & Despa, S. Intracellular Na⁺ regulation in cardiac myocytes. *Apr 01.* [https://doi.org/10.1016/S0008-6363\(02\)00656-9](https://doi.org/10.1016/S0008-6363(02)00656-9) (2003).
46. Molkentin, J. D. Calcineurin-NFAT signaling regulates the cardiac hypertrophic response in coordination with the MAPKs. *Aug 15* <https://doi.org/10.1016/j.cardiores.2004.01.021> (2004).
47. Williams, R. S. Calcineurin signaling in human cardiac hypertrophy. *May 14.* <https://doi.org/10.1161/01.CIR.0000017141.01845.FA> (2002).
48. Xia, H. et al. Na⁺/H⁺ Exchanger 1, a Potential Therapeutic Drug Target for Cardiac Hypertrophy and Heart Failure, Jul. 01, *MDPI*. (2022). <https://doi.org/10.3390/ph15070875>
49. Jiang, Y. et al. Radical scavenging and anti-inflammatory activities of (hetero)arylethenesulfonyl fluorides: synthesis and structure-activity relationship (SAR) and QSAR studies. *Bioorg. Chem.* **89**, 103015. <https://doi.org/10.1016/j.bioorg.2019.103015> (2019).
50. Stams, T. et al. Structures of murine carbonic anhydrase IV and human carbonic anhydrase II complexed with Brinzolamide: molecular basis of isozyme-drug discrimination. *Protein Sci.* **7** (3), 556–563. <https://doi.org/10.1002/pro.5560070303> (1998).
51. Dong, Y. et al. Structure and mechanism of the human NHE1-CHP1 complex. *Nat. Commun.* **12** (1). <https://doi.org/10.1038/s41467-021-23496-z> (Dec. 2021).
52. Shivakumar, D. et al. Prediction of absolute solvation free energies using molecular dynamics free energy perturbation and the OPLS force field. *J. Chem. Theory Comput.* **6** (5), 1509–1519. <https://doi.org/10.1021/ct900587b> (May 2010).
53. Jyothi, M., Khamees, H. A., Patil, S. M., Ramu, R. & Khanum, S. A. Microwave-Assisted synthesis, characterization, Docking studies and molecular dynamic of some novel phenyl thiazole analogs as Xanthine oxidase inhibitor. *J. Iran. Chem. Soc.* **19** (9), 3919–3933. <https://doi.org/10.1007/s13738-022-02574-z> (2022).
54. Greenidge, P. A., Kramer, C., Mozziconacci, J. C. & Wolf, R. M. Successes, Failures, and Directions for Further Improvement. *J. Chem. Inf. Model.* **53** (1), 201–209. <https://doi.org/10.1021/ci300425v> (Jan. 2013). MM/GBSA Binding Energy Prediction on the PDBbind Data Set.
55. Li, J. et al. The VSGB 2.0 model: A next generation energy model for high resolution protein structure modeling. *Proteins Struct. Funct. Bioinform.* **79** (10), 2794–2812. <https://doi.org/10.1002/prot.23106> (Oct. 2011).
56. Suryakoppa, K. S., Kameshwar, V. H., Appadurai, R., Eranna, S. & Khan, M. H. M. Enantiomeric Separation of Indole-3-Propanamide Derivatives by Using Supercritical Fluid Chromatography on a Polysaccharide-Based Chiral Stationary Phase, *J Chromatogr Sci*, vol. 60, no. 7, pp. 692–704, Sep. (2022). <https://doi.org/10.1093/chromsci/bmab102>
57. Ho, Y. T. et al. Jun., Inhibition of carbonic anhydrase II by steroidal and non-steroidal sulphamates, *Biochem Biophys Res Commun*, vol. 305, no. 4, pp. 909–914, (2003). [https://doi.org/10.1016/S0006-291X\(03\)00865-9](https://doi.org/10.1016/S0006-291X(03)00865-9)
58. DH, H. S., Sultana, R., Prabhu, A., Mohanto, P. S. R. S. & Subramaniyan, V. Biomedicine and pharmacotherapeutic effectiveness of combinatorial Atorvastatin and Quercetin on diabetic nephropathy: an in vitro study. *Biomed. Pharmacotherapy.* **174** <https://doi.org/10.1016/j.biopha.2024.116533> (May 2024).

59. Pavan, S. R. & Prabhu, A. Novel pH responsive hesperidin nanoformulation exerts anticancer activity on lung adenocarcinoma cells by targeting Akt/mTOR and MEK/ERK pathways. *J. Mater. Res.* **39** (8), 1217–1231. <https://doi.org/10.1557/s43578-024-01304-w> (2024).
60. Meduri, B. et al. New LPA1 receptor modulators: design, synthesis, in-silico, and anticancer studies of Triazole and oxadiazole analogs. *J. Mol. Struct.* **1295**, 136672. <https://doi.org/10.1016/j.molstruc.2023.136672> (2024).
61. Li, R. et al. MIR-7a/b attenuates post-myocardial infarction remodeling and protects H9c2 cardiomyoblast against hypoxia-induced apoptosis involving Sp1 and PARP-1. *Sci. Rep.* **6** <https://doi.org/10.1038/srep29082> (Jul. 2016).
62. huai Hu, Y. et al. Sep., sFRP1 protects H9c2 cardiac myoblasts from doxorubicin-induced apoptosis by inhibiting the Wnt/PCP-JNK pathway, *Acta Pharmacol Sin.*, vol. 41, no. 9, pp. 1150–1157, (2020). <https://doi.org/10.1038/s41401-020-0364-z>
63. Zweifach, A. Samples in many cell-based experiments are matched/paired but taking this into account does not always increase power of statistical tests for differences in means. *Mol. Biol. Cell.* **35** (1), br1. <https://doi.org/10.1091/mbc.E23-05-0159> (Jan. 2024).

Acknowledgements

The authors thank Department of Science and Technology, Ministry of Science and Technology, India, and JSS Academy of Higher Education and Research for the financial support, JSS Academy of Higher Education and Research, and Yenepoya Research Centre Yenepoya (Deemed to be University) for providing laboratory facilities.

Author contributions

J.M.S. and M.M., developed the research idea; M.M., S.G.P., P.S.R., and N.S.D., performed all laboratory experiments, and M.M., C.S., V.H.K., performed and analyzed computational experiments; J.M.S., M.M., S.D., V.H.K., T.S.K., C.S., and S.K.P., contributed to the design of the study, and evaluation of the results, and J.M.S., M.M., S.D., V.H.K., T.S.K., C.S., S.K.P., S.F.A., and S.M.A., contributed in writing and revising the manuscript. All authors have read and approved the manuscript.

Funding

Research supported by Department of Science and Technology (DST-SERB), Ministry of Science and Technology, Government of India, New Delhi (SRG/2021/001016), JSS Academy of Higher Education and Research, Mysuru (JSSAHER/REG/RES/URG/54/2023-24 and JSSAHER/REG/RES/URG/54/2011-12/7951), and King Saud University, Riyadh, Saudi Arabia, Project Number (RSPD2024R709).

Declarations

Competing interests

The authors declare no competing interests.

Additional information

Supplementary Information The online version contains supplementary material available at <https://doi.org/10.1038/s41598-025-95537-2>.

Correspondence and requests for materials should be addressed to S.D. or J.M.S.

Reprints and permissions information is available at www.nature.com/reprints.

Publisher's note Springer Nature remains neutral with regard to jurisdictional claims in published maps and institutional affiliations.

Open Access This article is licensed under a Creative Commons Attribution-NonCommercial-NoDerivatives 4.0 International License, which permits any non-commercial use, sharing, distribution and reproduction in any medium or format, as long as you give appropriate credit to the original author(s) and the source, provide a link to the Creative Commons licence, and indicate if you modified the licensed material. You do not have permission under this licence to share adapted material derived from this article or parts of it. The images or other third party material in this article are included in the article's Creative Commons licence, unless indicated otherwise in a credit line to the material. If material is not included in the article's Creative Commons licence and your intended use is not permitted by statutory regulation or exceeds the permitted use, you will need to obtain permission directly from the copyright holder. To view a copy of this licence, visit <http://creativecommons.org/licenses/by-nc-nd/4.0/>.

© The Author(s) 2025